MedChemComm

RESEARCH ARTICLE

View Article Online
View Journal

Cite this: DOI: 10.1039/c6md00573j

Discovery of decamidine as a new and potent PRMT1 inhibitor†‡

Jing Zhang,§[a] Kun Qian,§[a] Chunli Yan,[b] Maomao He,[a] Brenson A. Jassim,[a] Ivaylo Ivanov[b] and Yujun George Zheng*[a]

Received 13th October 2016,
Accepted 30th December 2016

DOI: 10.1039/c6md00573j

www.rsc.org/medchemcomm

Protein arginine methyltransferase 1 (PRMT1) is a key player for the dynamic regulation of arginine methylation. Its dysregulation and aberrant expression are implicated in various pathological conditions, and a plethora of evidence suggests that PRMT1 inhibition is of significant therapeutic value. Herein, we reported the modification of a series of diamidine compounds with varied lengths in the middle alkyl linker for PRMT1 inhibition. Decamidine (**2j**), which possesses the longest linker in the series, displayed 2- and 4-fold increase in PRMT1 inhibition (IC_{50} = 13 μM), compared with furamidine and stilbamidine. The inhibitory activity toward PRMT1 was validated by secondary orthogonal assays. Docking studies showed that the increased activity is due to the extra interaction of the amidine group with the SAM binding pocket, which is absent when the linker is not long enough. These results provide structural insights into developing the amidine type of PRMT1 inhibitors.

1. Introduction

Epigenetic regulation, mainly composed of DNA methylation and histone modifications such as methylation and acetylation, plays an essential role in eukaryotic life and contributes to a plethora of pathological conditions such as cancer. The concept of epigenetic alternations being an important cause of tumor initiation, progression and metastasis has prompted intense study on the development of epigenetic drugs which is best represented by the approval of two histone deacetylase (HDAC) inhibitors (vorinostat and romidepsin) for the treatment of cutaneous T-cell lymphoma.[1–3] Besides acetylation, histone arginine methylation is another significant epigenetic player in this anti-cancer arena. Overexpression of protein arginine methyltransferase 1 (PRMT1), which is the major enzyme catalyzing monomethylation and asymmetric dimethylation of arginine residues of protein substrates, has been linked with various cancer phenotypes, including leukemia, lung, prostate, and breast cancers.[4] Application of PRMT1 inhibitors or inactivation of PRMT1 by siRNA, has great potential to significantly hamper tumor cell growth.[5–8]

So far, a handful of PRMT1 inhibitors have been discovered or designed.[7,9–15] Diamidine compounds represent one of the best studied PRMT1 inhibitors. The compound stilbamidine (Fig. 1),[15] which was discovered by the Jung group, is the first diamidine compound with potent PRMT1 inhibitory activity. As a result of PRMT1 inhibition, histone hypomethylation was induced while estrogen receptor activation was reduced by this compound in functional assays.[15] Focused library screening by our group identified the compound furamidine (DB75) and its analogs as low micromolar PRMT1 inhibitors. The compound furamidine possessed a two-fold lower IC_{50} value compared with stilbamidine, and it showed >10-fold selectivity over the other PRMTs including PRMT5. Supported by structural modelling, the amidine groups in both stilbamidine and furamidine most likely mimic the guanidino moiety of the arginine residue, and this concept is also confirmed by the mechanistic study showing that the compound furamidine is partially competitive towards the substrate and noncompetitive towards the

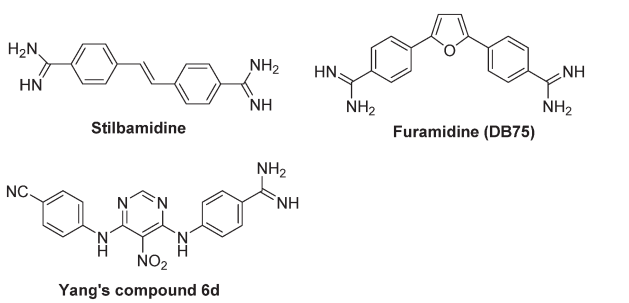

Fig. 1 Reported PRMT1 inhibitors which contain the amidine functionality.

[a] Department of Pharmaceutical and Biomedical Sciences, College of Pharmacy, The University of Georgia, Athens, Georgia 30602, USA. E-mail: yzheng@uga.edu
[b] Department of Chemistry, Center for Diagnostics and Therapeutics, Georgia State University, Atlanta, Georgia 30302, USA

† The authors declare no competing interests.

‡ Electronic supplementary information (ESI) available. See DOI: 10.1039/c6md00573j

§ Jing Zhang and Kun Qian contributed equally.

cofactor.[7] Recently the SAR study of amidine compounds by Yu *et al.* confirmed the importance of the amidine group, showing that its deletion ablates PRMT1 inhibition.[11] In that study, the researchers identified compound **6d** (Fig. 1) as a potent PRMT1 inhibitor with an IC_{50} of 2.0 μM.

In our continuing studies on structural modifications of diamidine compounds, we found that slightly varying the linkers in stilbamidine can be tolerated (data not shown). This inspired us to explore other diamidine compounds with varied lengths of the middle linker such as pentamidine, which was reported to be a DNA binder and has been clinically used as an antiparasitic drug in a similar manner to furamidine.[16,17] In this study, we set up a facile synthesis of amidine analogs with different hydrocarbon linkers between the two benzamidine moieties. The activities of these compounds on PRMT1 inhibition were studied with biochemical assays. The most active compound **2j** was docked into the active site of PRMT1 to decipher the structural basis for the linker length influence on the potencies of the inhibitors.

2. Results and discussion

The compounds phenamidine (**2a**) and pentamidine (**2h**) were obtained commercially. The other compounds were synthesized using the synthetic route illustrated in Scheme 1. First, commercially available 4-cyanophenol was reacted with an excess of dibromo- or dichloro-alkane under basic conditions to yield the alkoxylbenzonitrile compounds **1**. Classically, the cyano groups in these compounds could be converted to amidine groups *via* the Pinner reaction through an imino ether intermediate followed by the addition of ammonia in ethanol.[18] However, we noticed incomplete conversion and a low yield by this method (data not shown). Therefore, an easier method under basic conditions was investigated. In this method, the intermediate **1** was treated in LiHMDS (lithium bis(trimethylsilyl)amide, 1 N in tetrahydrofuran) at room temperature overnight, followed by quenching with 2 N HCl solution. This method allowed complete conversion of the cyano group to amidine, and therefore led to high yields. Meanwhile, the reaction is not sensitive to moisture, so it is suitable for small-scale reaction and can be easily handled. The crude product can be purified by precipitation from H_2O, or by preparative HPLC if needed. The purity and identity of the compounds were validated by NMR and mass spectrometry (see the ESI‡).

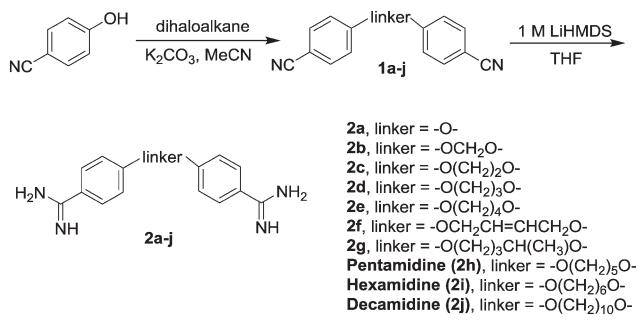

Scheme 1 Synthetic route to diamidine compounds.

The PRMT1 inhibitory activities of compounds **2a–2j** were evaluated by using our previously established scintillation proximity assay (SPA),[19] which measured the amount of methyl transfer from [^{3}H]-SAM to biotinylated histone H4 peptide (ac-SGRGKGGKGLGKGGAKRHRK(Biotin)-NH_2, abbreviated as H4-20-Biotin). Furamidine was also used as a positive control. As shown in Fig. 2, there was no significant difference in PRMT1 inhibition among compounds **2a–2g**, with the residual PRMT1 activity ranging from 80% to 57%. Therefore, the middle methylene length in the range of 0–4 (referring to the numbers of methylene units) was not particularly sensitive to PRMT1 binding under the current assay conditions. However, when the carbon length increased to above 5 methylene units, the PRMT1 inhibition difference was distinct enough to be observed following the ranking order of **2j** (decamidine) > **2i** (hexamidine) > **2h** (pentamidine), suggesting that the potency for PRMT1 inhibition increases as the middle linker elongates to above 5.

To determine whether the tested diamidine compounds were specific for PRMT1, we also screened the inhibitory activities of these compounds against PRMT5, the major type II PRMT enzyme. As shown in Fig. 3, the majority of diamidine compounds did not show significant PRMT5 inhibition, except for compounds **2b**, **2j** and furamidine, which showed *ca.* 50% inhibition at 100 μM.

Then, the IC_{50} values in PRMT1 inhibition were determined for compounds **2h–2j**, furamidine and stilbamidine with dose-dependent assays. A typical inhibition curve is shown in Fig. 4. As displayed in Table 1, consistent with the single-dose inhibition profile, the IC_{50} values of **2h**, **2i** and **2j** showed a decreasing trend with 81 μM, 52 μM and 13 μM, respectively. It should be noted that compound **2j** is more potent than furamidine, which showed an IC_{50} value of 22 μM under these experimental conditions. Interestingly, compared with furamidine, compound **2j** displayed a reduced selectivity over PRMT5 with an IC_{50} value of 43 μM.

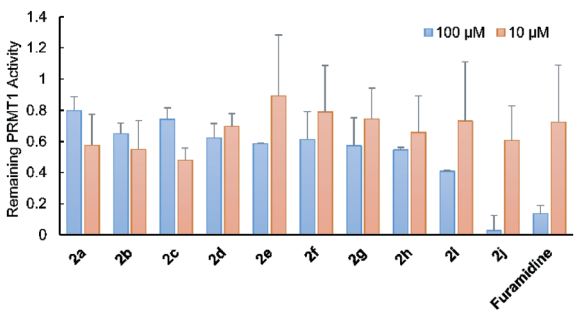

Fig. 2 PRMT1 inhibition of compounds **2a–2j** and furamidine at 100 μM and 10 μM concentrations. The reaction buffer contains 50 mM HEPES, 10 mM NaCl, 0.5 mM EDTA and 0.5 mM DTT, and has pH 8.0. The concentrations of PRMT1, [^{3}H]-SAM, and H4-20-Biotin are 0.01, 0.5, and 0.5 μM, respectively. The mixtures were incubated at room temperature for 15 min.

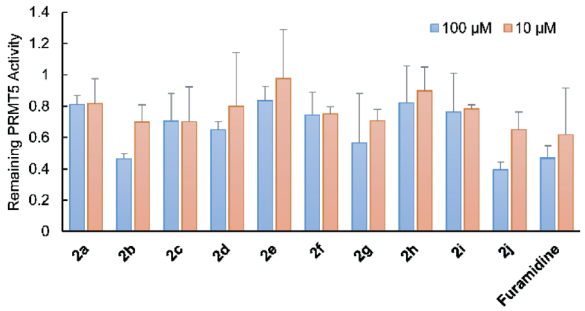

Fig. 3 PRMT5 inhibition of compounds **2a–2j** and furamidine at 100 μM and 10 μM concentrations. The reaction conditions were similar to those Fig. 2, except that the reaction time was 45 min.

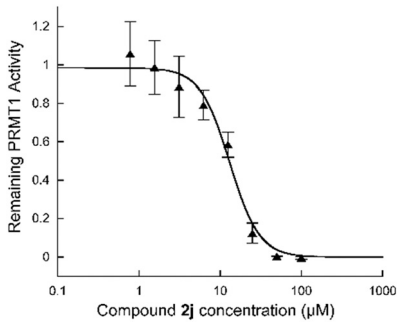

Fig. 4 The dose-dependent PRMT1 inhibition curve by compound **2j**.

Table 1 IC_{50} values of selected compounds for PRMT1 and PRMT5

Compounds	IC_{50}, μM	
	PRMT1	PRMT5
Stilbamidine	52 ± 2	712 ± 161
Furamidine	22 ± 2	256 ± 1
Pentamidine (**2h**)	81 ± 3	582 ± 100
Hexamidine (**2i**)	52 ± 3	357 ± 155
Decamidine (**2j**)	13 ± 1	43 ± 1

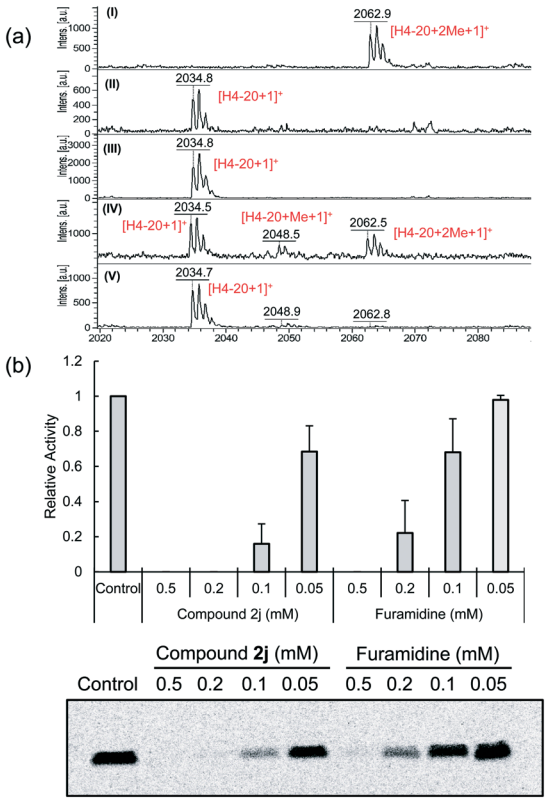

Fig. 5 The comparison of PRMT1 inhibition by compounds **2j** and furamidine. (a) Mass spectra of the reaction mixture with different concentrations of compounds **2j** and furamidine. From spectra I to V: DMSO control, compound **2j** (0.2 mM), compound **2j** (0.5 mM), furamidine (0.2 mM), furamidine (0.5 mM). The concentrations of PRMT1, SAM, and H4-20 were 1, 200, and 50 μM, respectively. The mixtures were incubated at 30 °C for 3.5 h. (b) Radiometric gel assay and its quantification. The concentrations of PRMT1, [^{14}C]SAM, and H4-20 are 0.1, 20, and 100 μM, respectively. The reaction time was 30 min at 30 °C before it was quenched with 5 × SDS-loading buffer, separated by 15% SDS-PAGE, dried under vacuum and visualized by storage phosphorimaging. The quantification was based on two experiments.

To further validate the PRMT1 inhibition by **2j**, mass spectrometric analysis of the methylation reaction mixture using regular SAM was conducted. As shown in the spectrum I in Fig. 5a, the substrate histone 4 (1–20) with N-terminal acetyl group (abbreviated as H4-20) was completely converted to dimethyl H4-20 in the absence of any inhibitor. However, when compound **2j** was added at 0.2 mM or 0.5 mM concentrations (spectra II and III in Fig. 5a), this methyl transfer reaction was completely inhibited, showing that only H4-20 was detected in the reaction mixture. In comparison, when furamidine was used for inhibition, the MALDI result showed that both H4-20 and dimethyl H4-20 were detected at 0.2 mM concentration (spectra IV in Fig. 5a), suggesting an incomplete inhibition. We also examined the inhibition effect with the radiometric gel assay. In this assay, different concentrations of inhibitors were incubated with PRMT1, H4-20 and [^{14}C]SAM. The reaction mixture was resolved on a 15% SDS-PAGE gel. The gel was vacuum dried and then subjected to phosphorimaging detection. As shown in Fig. 5b, no methylation was observed when compound **2j** was at 0.2 mM. However, methylation was still observed at the same concentration of furamidine. Quantitation analysis revealed that the extent of methylation with compound **2j** at 0.1 and 0.05 mM was very similar to that with furamidine at 0.2 and 0.1 mM, consistent with the IC_{50} measurement in which compound **2j** was two-fold more potent than furamidine.

Evidently, elongating the middle linker could significantly enhance the potency of diamidine compounds for PRMT1 inhibition, resulting in compound **2j** being more potent than furamidine. To probe possible structural differences in the PRMT1-inhibitor interaction at different linker lengths, compounds **2i** and **2j** were docked into a homology model of PRMT1 using Autodock4.2 as described in our previous work.[7] The docking scores for compounds **2i** and **2j** were −10.1 and −11.0 kcal mol^{-1}, respectively. Therefore, compound **2j** can form an energetically more favorable

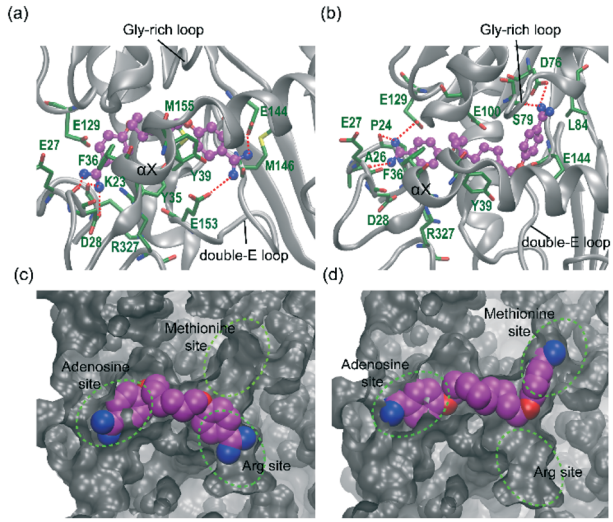

Fig. 6 Predicted conformation of **2i** and **2j** bound to PRMT1 from docking. (a) Detailed view of **2i** displaying the key PRMT1 residues. (b) Detailed view of **2j** displaying the key PRMT1 residues. The PRMT1 homology structure was constructed by using the known structure of *R. norvegicus* PRMT3 (PDB code: 1F3L[20]) and *H. sapiens* PRMT3 (PDB code: 3SMQ[21]). Compounds **2i** and **2j** are shown in a magenta ball and stick representation. The PRMT1 residues involved in binding to **2i** and **2j** are shown as green sticks and labeled. The red dashed lines represent hydrogen bonds. (c) Shape of the binding cavity of PRMT1 (grey) with **2i** (magenta sphere). (d) Shape of the binding cavity of PRMT1 (grey) with **2j** (magenta sphere). The surface in panels (c) and (d) is visualized with VMD.[22]

interaction with PRMT1, which is in accordance with biological activity results. As shown in Fig. 6a and c, the diamidine moiety of **2i** inserts into both the SAM adenosine binding site and the Arg substrate site analogous to the previously reported binding mode of furamidine to PRMT1.[7] Moreover, the docking analysis shows that one of the amidine groups of **2i** forms three favorable hydrogen bonds: one with residue P24 and two with the backbone carbonyl groups of residues K23 and E27. The second amidine group of **2i** is stabilized *via* hydrogen bonds to the side chains of E144 and E153 (two important residues in the double-E loop). For compound **2j**, the first amidine group occupies the same SAM adenosine site as in the **2i** complex (*via* two hydrogen bonds to the backbone carbonyl group of P24 and A26, a hydrogen bond with the side chain of E129). However, the binding pattern for the second amidine group of **2j** is completely different. In the case of **2j**, the flexible 10-carbon linker can stretch and position this amidine group into the cofactor methionine binding site. In this orientation, the amidine interacts with the Gly-rich loop of PRMT1 (residues G78 and G80) through hydrogen bonds with the side chain of D76 and the backbone carbonyl group of S79. The deep placement of the amidine in the cofactor pocket with multiple interactions formed accounts for the stronger binding of **2j** with PRMT1 (Fig. 6d).

The different binding mode for the second amidine group could explain the origin of the differences in the observed activity of **2i** and **2j**. The phenyl rings and the linker of **2i** and **2j** also form hydrophobic interactions with the side chain of F36 and Y39, including π–π interactions (T-shape geometry) from the N-terminal αX helix, which forms the roof of the pocket above the ligand. These interactions thus tightly anchor **2i** and **2j** in the PRMT1 active site. Docking of **2i** and **2j** also suggests that both compounds are nestled to allow good shape complementarity to the cavity formed by the adjacent substrate/cofactor sites in PRMT1 (Fig. 6c and d).

To probe the selectivity difference between compounds **2i** and **2j**, we also docked both compounds with PRMT5. As can be seen in Fig. S1,‡ both compounds only bind to the cofactor site of PRMT5. For compound **2i**, it spans both the cofactor and arginine sites for PRMT1, but only the cofactor site for PRMT5. For compound **2j**, it binds to PRMT1 and PRMT5 similarly. This may partially explain the low selectivity of this compound.

3. Conclusions

The results of the present study demonstrate that diamidine compounds are capable of inhibiting the methyl transfer activity of PRMT1 with varied potencies. Among the analogs with different lengths of linkers (C0–C6, C10), the potency of inhibition increased as the linker length increased, and the most potent inhibitor was compound **2j** (decamidine) with a C10 linker. Compared with stilbamidine and furamidine, this compound showed moderately increased PRMT1 inhibition, but slightly decreased selectivity against PRMT5. Besides the potency characterization using the SPA measurement, the inhibitory activity of **2j** was also confirmed by mass spectrometry analysis of the reaction mixture and gel phosphorimaging assay. The increased PRMT1 inhibition could be attributed to the occupation by the amidine group of the SAM binding site which resulted from the extension of the middle linker. In order to reach this extra interaction, the linker needs to be long enough to stretch out, and a linker length of over five methylene groups appears to be the threshold for transitioning from one binding mode to the other. Future work is warranted for detailed investigation of diamidine compounds in cellular PRMT1 activity inhibition as well as correlating biochemical potencies with potential anti-cancer activities in PRMT1 overexpressed tumor models. Compound **2j** with a C10 linker could be an interesting hit for further optimization by finely tuning the length of the hydrocarbon linker and the substitutions of the phenyl rings. Our effort towards these directions will be reported in due time.

Acknowledgements

This work was supported by the National Institute of Health Grant R01GM086717 to Y. G. Z. and R01GM110387 to I. I. Jing Zhang was supported by American Heart Association Postdoctoral Fellowship # 16POST27260147. The authors acknowledge the Proteomics and Mass Spectrometry (PAMS) Facility at UGA for the MS support, and Dr. D. Cui of the Chemistry department at UGA for NMR assistance.

References

1 S. Rangwala, C. Zhang and M. Duvic, *Future Med. Chem.*, 2012, **4**, 471–486.
2 O. Khan and N. B. La Thangue, *Immunol. Cell Biol.*, 2012, **90**, 85–94.
3 S. Jain, J. Zain and O. O'Connor, *J. Hematol. Oncol.*, 2012, **5**, 24.
4 Y. Yang and M. T. Bedford, *Nat. Rev. Cancer*, 2013, **13**, 37–50.
5 M. Yoshimatsu, G. Toyokawa, S. Hayami, M. Unoki, T. Tsunoda, H. I. Field, J. D. Kelly, D. E. Neal, Y. Maehara, B. A. Ponder, Y. Nakamura and R. Hamamoto, *Int. J. Cancer*, 2011, **128**, 562–573.
6 J. Wang, L. Chen, S. H. Sinha, Z. Liang, H. Chai, S. Muniyan, Y. W. Chou, C. Yang, L. Yan, Y. Feng, K. K. Li, M. F. Lin, H. Jiang, Y. G. Zheng and C. Luo, *J. Med. Chem.*, 2012, **55**, 7978–7987.
7 L. Yan, C. Yan, K. Qian, H. Su, S. A. Kofsky-Wofford, W. C. Lee, X. Zhao, M. C. Ho, I. Ivanov and Y. G. Zheng, *J. Med. Chem.*, 2014, **57**, 2611–2622.
8 N. Cheung, T. K. Fung, B. B. Zeisig, K. Holmes, J. K. Rane, K. A. Mowen, M. G. Finn, B. Lenhard, L. C. Chan and C. W. So, *Cancer Cell*, 2016, **29**, 32–48.
9 H. Hu, K. Qian, M. C. Ho and Y. G. Zheng, *Expert Opin. Invest. Drugs*, 2016, **25**, 335–358.
10 E. M. Bissinger, R. Heinke, A. Spannhoff, A. Eberlin, E. Metzger, V. Cura, P. Hassenboehler, J. Cavarelli, R. Schule, M. T. Bedford, W. Sippl and M. Jung, *Bioorg. Med. Chem.*, 2011, **19**, 3717–3731.
11 X. R. Yu, Y. Tang, W. J. Wang, S. Ji, S. Ma, L. Zhong, C. H. Zhang, J. Yang, X. A. Wu, Z. Y. Fu, L. L. Li and S. Y. Yang, *Bioorg. Med. Chem. Lett.*, 2015, **25**, 5449–5453.
12 A. Spannhoff, R. Machmur, R. Heinke, P. Trojer, I. Bauer, G. Brosch, R. Schule, W. Hanefeld, W. Sippl and M. Jung, *Bioorg. Med. Chem. Lett.*, 2007, **17**, 4150–4153.
13 N. Fontan, P. Garcia-Dominguez, R. Alvarez and A. R. de Lera, *Bioorg. Med. Chem.*, 2013, **21**, 2056–2067.
14 M. S. Eram, Y. Shen, M. M. Szewczyk, H. Wu, G. Senisterra, F. Li, K. V. Butler, H. U. Kaniskan, B. A. Speed, C. dela Sena, A. Dong, H. Zeng, M. Schapira, P. J. Brown, C. H. Arrowsmith, D. Barsyte-Lovejoy, J. Liu, M. Vedadi and J. Jin, *ACS Chem. Biol.*, 2016, **11**, 772–781.
15 A. Spannhoff, R. Heinke, I. Bauer, P. Trojer, E. Metzger, R. Gust, R. Schule, G. Brosch, W. Sippl and M. Jung, *J. Med. Chem.*, 2007, **50**, 2319–2325.
16 F. C. Bocobo, A. C. Curtis and E. R. Harrell, *J. Invest. Dermatol.*, 1953, **21**, 149–156.
17 V. Jean-Moreno, R. Rojas, D. Goyeneche, G. H. Coombs and J. Walker, *Exp. Parasitol.*, 2006, **112**, 21–30.
18 A. Pinner and F. Klein, *Ber. Dtsch. Chem. Ges.*, 1877, **10**, 1889–1897.
19 J. Wu, N. Xie, Y. Feng and Y. G. Zheng, *J. Biomol. Screening*, 2012, **17**, 237–244.
20 X. Zhang, L. Zhou and X. Cheng, *EMBO J.*, 2000, **19**, 3509–3519.
21 A. Siarheyeva, G. Senisterra, A. Allali-Hassani, A. Dong, E. Dobrovetsky, G. A. Wasney, I. Chau, R. Marcellus, T. Hajian, F. Liu, I. Korboukh, D. Smil, Y. Bolshan, J. Min, H. Wu, H. Zeng, P. Loppnau, G. Poda, C. Griffin, A. Aman, P. J. Brown, J. Jin, R. Al-Awar, C. H. Arrowsmith, M. Schapira and M. Vedadi, *Structure*, 2012, **20**, 1425–1435.
22 W. Humphrey, A. Dalke and K. Schulten, *J. Mol. Graphics*, 1996, **14**, 33–38.